DOI: ADD DOINUMBER HERE

Virtual pilot: a review of the human pilot's mathematical modeling techniques

Francesca Roncolini[⋆†] *and Giuseppe Quaranta*[⋆]
[⋆] *Politecnico di Milano, Department of Aerospace Engineering*
Via Privata Giuseppe La Masa, 34/B12, 20156 Milano MI
francesca.roncolini@polimi.it · giuseppe.quaranta@polimi.it
[†]Corresponding author

Abstract

This paper contains a review of the state of the art of virtual pilot modeling. The virtual pilot is a mathematical model of the behaviour of a trained human involved in a vehicle piloting task. These models are fundamental to perform closed-loop simulations. The models presented here are divided into frequency-based and time-based, and for each of them advantages and disadvantages are discussed in order to help the reader select a suitable model for a given task. The time-based models are found to be more adaptable and suitable for online characterization, while the frequency-based are easier to tune, but offline.

1. Introduction

Virtual prototypes and mathematical models are a powerful assessment instrument during several phases of the flying vehicle life-cycle, from the preliminary design to certification, as explained by Padfield.[15] Certain certification flight test activities, particularly those involving hazardous maneuvers, can be classified as high-risk in terms of flight safety, therefore the possibility to involve flight simulations in the certification process is currently widely evaluated.[16]
For instance, in this document by Avi et al.[1] is reported a proposed methodology to validate and certify Point-in-Space (PinS) helicopter routes using simulation: the GNSS signal level on the designated route and the presence of obstacles on the path can be checked by a small UAV, while the pilot's workload and the respect of the helicopter performance constraints can be assessed by means of closed-loop simulations where both the dynamics of the pilot and of the rotorcraft are modeled. The simulations would avoid:

1. the costs involved by a flight campaign to collect the necessary data, considering that there may be several iterations before finding a route compatible with the pilot's workload and the helicopter performance constraints;
2. the risks of performing this experimental activity without checking the range of workload and performance implied by the route beforehand.

As mentioned above, the closed-loop simulation model must contain both the dynamics of the helicopter, or vehicle in general, and of the pilot. It is therefore necessary, while approaching this task, to devote some effort to understanding how to properly model the human pilot and their interaction with the vehicle.
The purpose of the paper is to introduce the pilot dynamics modeling topic to researchers and engineers who may need to set up a closed-loop simulation environment and are still unfamiliar with the models, in order to help them orient themselves among the possible choices.

1.1 Passive vs. active pilot model

The pilot can be seen as:

- a passive element, which does not exert an intentional control action command, and who is instead a bio-dynamic element that closes the loop by simply keeping their hands on the control inputs: this type of model is useful to study some phenomena such as PAO (pilot-assisted oscillations) which are produced when the flying vehicle is subject to vibrations transferred by the seat to the pilot, who in turn transfers them to the vehicle through the control stick involuntarily[11] ;

- an active element, who exerts a voluntary control action on the vehicle by means of the control inputs.

In this paper the pilot is intended as an active control element. The human operator will be treated as the controller that closes the aircraft dynamics loop.

1.2 Fundamental concepts about the pilot

The AGARD report by McRuer and Krendel[14] reports three fundamental concepts regarding the pilot-in-the-loop systems:

- The pilot establishes appropriate control loops around the aircraft, which by itself could not accomplish the necessary tasks;
- The pilot acts as an adaptive controller that suits its gains to the aircraft dynamics, achieving the aircraft stabilization and enhancing its performance;
- The cost of the pilot's adaption is the workload-induced stress and the reduced potential to cope with the unexpected.

The concept of the pilot being an adaptive controller is the key to a proper modelling of the pilot's behaviour. However, it must be taken into account that pilots are subjected to individual differences, also known as "pilot-centered variables", such as the personal piloting style (aggressive or not), the physical condition, the training, that can contribute to a certain variability in the pilot gains and delays. This variability becomes confined to a very tight band when performance demands become constraining or when the aircraft dynamics is strongly unstable.

1.3 Pilot modeling techniques

The research into the modeling of the human pilot's control behaviour started in the 1940's, and from then until the 1960's it was focused on single-input-single-output systems analyses using frequency domain models coming from the classical control theory.[12]
In 1970 took place the first attempt to describe the human pilot dynamics in the time domain, according to modern control techniques: the pilot was modelled as an optimal controller subject to human limitations. The model proposed by Kleinman, Baron and Levinson[9] in 1970 is indeed called optimal control model (OCM).
Both the modeling fashions, frequency-based and time-based, were further developed in the following decades. The frequency-based pilot models can be split into two categories: the *behavioral-based*, which define an approximate pilot transfer function basing on the shape of the man-machine open loop transfer function observed experimentally, and the *iso-morphic*, which precisely define each component of the human perception and actuation chain. The time-based models are *algorithmic*, because they rely on optimal control algorithms to compute the pilot's gains: they don't explicitly mimic the human behaviour or functions, but lay on the hypothesis of the pilot being an optimal adaptive controller.

1.4 Compensatory vs. pursuit display

In the process of selecting a pilot model it is important to understand the difference between compensatory and pursuit tasks, because some models are explicitly referred to one of the two tasks.
In compensatory tasks, the only information presented to the pilot through the display is the error between system output and desired output. The compensatory control logic is shown in Figure 1.

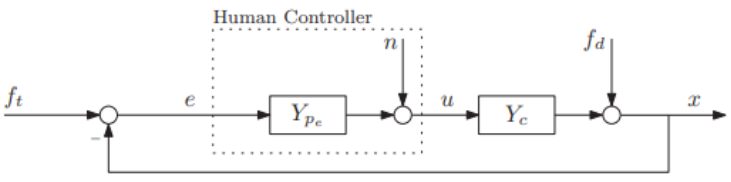

Figure 1: Compensatory control strategy

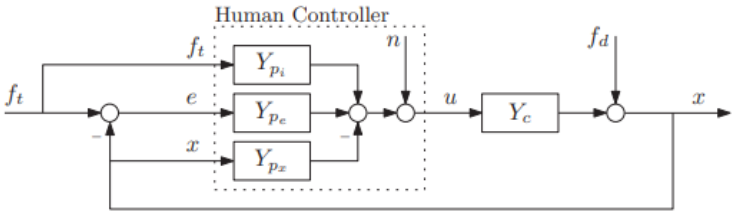

Figure 2: Pursuit control strategy

In pursuit tasks, the pilot can observe the system error, the system output and the desired output, therefore, having more information, they can choose a more complex control strategy. The pursuit control logic is shown in Figure 2.
The difference between compensatory and pursuit display is shown in Figure 3.

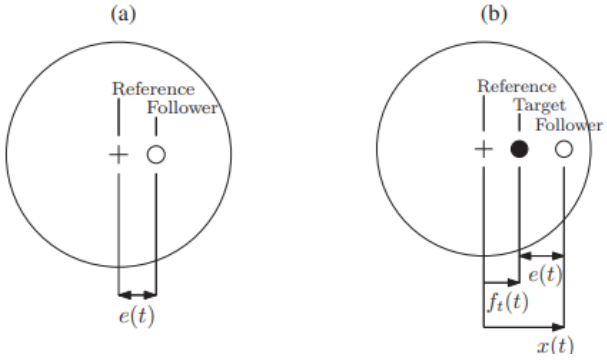

Figure 3: Compensatory and pursuit display

1.5 Outline of the paper

In the next sections, the main pilot models developed and currently used for closed-loop simulations are presented and discussed. For each model, one or more investigations that discuss validations or applications of the model are referenced, and a brief list of pros and cons is provided.

2. Pilot models

2.1 Frequency domain: behavioral-based

2.1.1 The crossover model

In the 1960's, Robert McRuer[14] proposed the principle called "crossover law", which is still considered the fundamental law in the man-machine interaction modeling. The concept at the base of this principle is that the pilot adjusts their control actions to comply with the controlled element dynamics.
The mathematical formulation of this principle in the frequency domain is the following:

$$Y_p(s)Y_c(s) = \frac{\omega_c}{s} exp(-\tau s) \tag{1}$$

or, if $Y_c(s)$ has slightly unstable poles λ:

$$Y_p(s)Y_c(s) = \frac{\omega_c}{s-\lambda} exp(-\tau s) \tag{2}$$

where Y_c is the controlled element (vehicle) transfer function, and Y_p is the pilot transfer function. Y_pY_c therefore is the open loop transfer function, as can be observed from the block diagram in Figure 4 (for the sake of simplicity, the display is not treated as a dynamic element). ω_c is the crossover frequency of the open loop transfer function, and τ is a time delay.

The crossover model is valid only in the neighborhood of ω_c.
By manipulation of Equation 1 it is possible to obtain the pilot transfer function in the crossover region:

$$Y_p(s) = Y_c^{-1}(s)\frac{\omega_c}{s}exp(-\tau s) \tag{3}$$

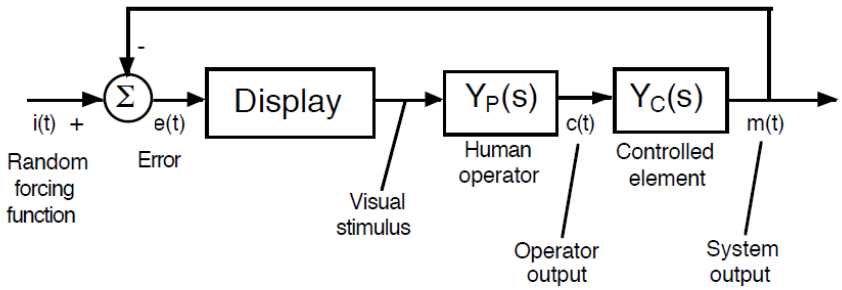

Figure 4: Pilot-vehicle block diagram

McRuer arrived to the elaboration of the crossover law by observing the operator output and system output produced by a random forcing function in several piloted systems with different controlled elements: the entire testing procedure is well described in the AGARD report[14] and is completely devoted to the characterization of compensatory tasks.
Equation 1 gives us important information about the behaviour of the pilot in the frequency domain: independently from the vehicle dynamics, the pilot maintains an open-loop transfer function slope of −20 dB/dec in the crossover frequency region. The operation of adjustment of the open-loop slope is called *equalization*.
However, the equalization process has a cost: the more lead the pilot has to generate in order to equalize and create the desired slope, the higher is the time delay τ from the visual stimulus to the operator output.

Parameters selection rules The rules to select the two parameters of this model, ω_c and τ, are illustrated in the 1967 document[13] by McRuer.
Here they are summarized, but for a better understanding the reader can refer to the above mentioned document.

Rule 1: *Equalization*. Given a controlled element transfer function of the type $Y_c = K_c \frac{\Sigma(1+\tau_{c_i}s)}{\Sigma(1+T_{c_i}s)}$, the pilot, whose goal is to set the open-loop amplitude slope to −20 dB/dec will have a general equalization transfer function $Y_{p_{eq}} = K_p \frac{\Sigma(1+\tau_{p_i}s)}{\Sigma(1+T_{p_i}s)}$: they must apply some leads and some lags in order to perform equalization. K_p is called the pilot gain, and the rest of the transfer function is called equalization term. A human pilot has obviously some physical limitations, and it was observed that they are not able to apply more than a lead and a lag at a time, therefore the equalization term will have the form $\frac{1+\tau_p s}{1+T_p s}$.
The poles and zeros of the pilot transfer function can be computed by imposing the open loop transfer function slope to −20 dB/dec in the crossover region.
From Equation 1, it will result that $K_c K_p = \omega_c$: K_p can be computed from the vehicle gain and from the crossover frequency.
The crossover frequency is computed according to the following rules.

Rule 2: *Delay*. According to the analyses performed in the AGARD document,[14]

$$\tau = \tau_0 - \Delta\tau(\omega_i) \tag{4}$$

where ω_i is the bandwidth of the forcing function (that is the closed-loop system input, or, in other terms, the desired closed-loop output).
$\Delta\tau$ depends uniquely on ω_i according to the graph shown in Figure 5.
τ_0 depends on the amount of lead required: by knowing the lead units required to the pilot, it is possible to compute τ_0 as indicated in Figure 6.

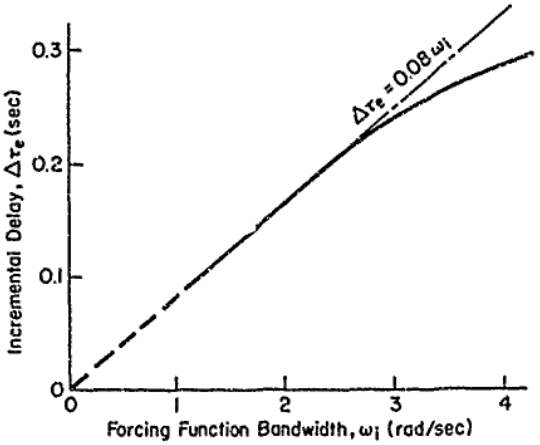

Figure 5: $\Delta\tau$ dependence on the forcing function bandwidth

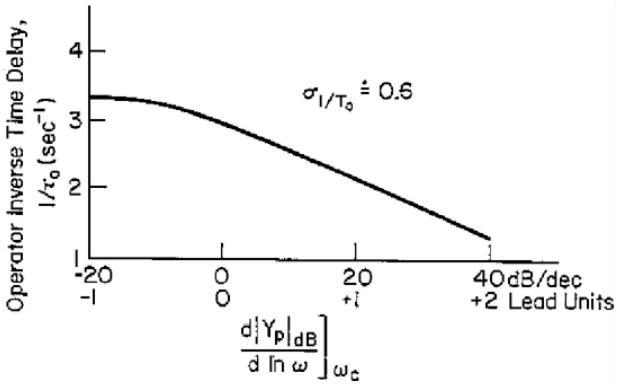

Figure 6: τ_0 dependence on the amount of lead performed by the pilot

Rule 3: *Crossover frequency* The crossover frequency, similarly to the delay, is the sum of two contributions:

$$\omega_c = \omega_{c_0} + \Delta\omega(\omega_i) \tag{5}$$

In first approximation, the $\Delta\omega(\omega_i)$ term can be neglected. In the AGARD document[14] it is proved that:

$$\omega_{c_0}\tau_0 = \frac{\pi}{2} \tag{6}$$

therefore, from Equation 6 it is possible to obtain $\omega_c = \frac{\pi}{2\tau_0}$ and consequently to compute the pilot gain K_p and fully characterize the crossover pilot model, that will be:

$$Y_p(s) = K_p \frac{(1 + \tau_p s)}{(1 + T_p s)} exp(-\tau s) \tag{7}$$

Remnant The crossover model of the human pilot as explained up to now appears to be a linear model. Actually, it was clear from the beginning to McRuer, while analyzing the data, that a noise component uncorrelated with the system input emerges in the pilot's output: this component is interpreted as a nonlinearity in the human pilot which cannot be modeled by the linear crossover model, and is called the remnant.
Therefore, the complete crossover model is composed by a linear component (Equation 1) and a nonlinear component (the remnant, often treated as a white noise): it is a quasi-linear model.

Pros and cons The crossover model is the fundamental law of human-machine interaction. However, it has some flaws: it is an extremely simplified model, which is valid only in the region of the crossover frequency. For instance, at low frequency the phase of the crossover model is proved to be quite different from the experimental open-loop phase.

It is therefore suggested to improve the quality and complexity of the model by adding some iso-morphic items, which model some of the real human dynamics, such as the neuromuscular system, for example. By doing so, the pilot gains will still be computed by means of the crossover model, but there will be additional dynamics which make the model more realistic.
The crossover law was tested and proved to be reliable only for single-axis and single-loop tasks, i.e. when the pilot directly controls the attitude on one axis.

2.2 Frequency domain: iso-morphic

2.2.1 The structural model

In 1980, R.A. Hess[4] provided a more realistic representation of the pilot's behaviour in compensatory tasks with respect to the quasi-linear crossover model.
He aimed at describing the underlying structure which contributes to human pilot dynamics, and that results in the crossover law.
The model, presented in Figure 7 is divided into central nervous system and neuromuscular system components, a division that emphasizes the nature of the signal processing activity involved.
As schematized in the figure, the model includes a display dynamics Y_{d_e}, through which the error is delivered to the

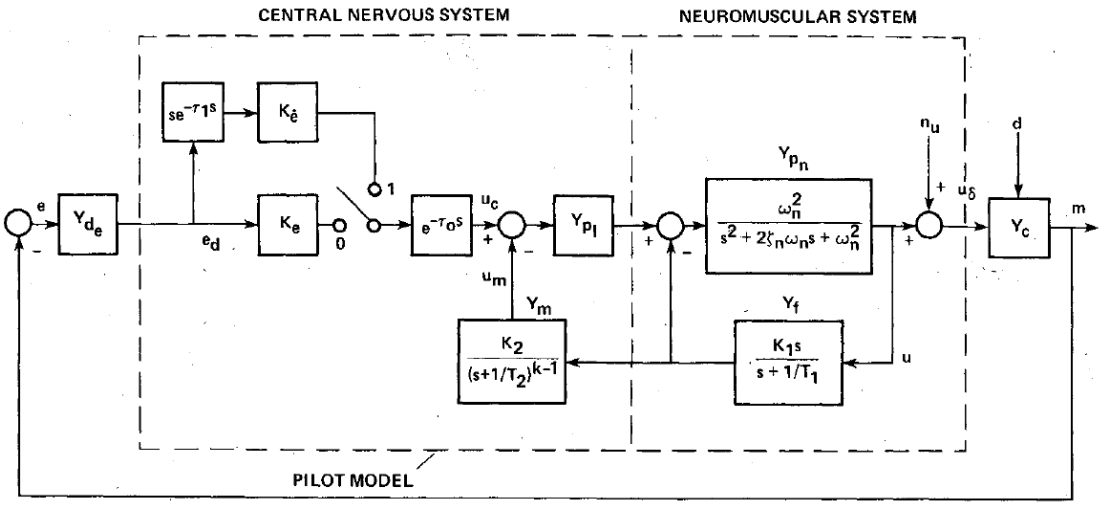

Figure 7: Structural model of the adaptive human pilot

pilot, who controls both the error and the error rate. The pilot performs an internal derivation of the error in order to obtain the error rate, and the cost of the derivation is a delay τ_1, which typical value is 0.2 s.
The control strategy switches from error to error rate in a casual manner, with an associated probability P_1 of the switch being in position 1 (error rate control).
Y_{p_l} contains a closed loop that models the pulsing logic through which the pilot faces high order controlled elements. A model of the pulsing logic is offered in another work by Hess.[3] If the controlled element has a standard dynamics up to the second order, this element can be put to 1.
τ_0 is the processing delay, which takes into account the latency of the visual process (average value: 0.075 s), the motor nerve conduction time (average value: 0.03 s) and the central processing time (average value: 0.03 s). Therefore τ_0 can be set to 0.14 s.
The form of the neuromuscular open-loop dynamics is based upon electromyogram measurements performed by Magdaleno et al.,[10] which establish that $\omega_n = 10$ rad/s and $\xi_n = 0.707$. The input of the neuromuscular system is the change in the average firing rate of the α motor neurons. The output is the motion of the control stick.
Y_f represents the feedback dynamics of the spindles in the limb driving the control stick. The spindles are basically length transducers that measure the extension of a muscle and provide the brain with a measurement of the motion performed by the limb. The closed loop is therefore needed to correct the position of the limb on the manipulator. K_1 can be put to 1.
Y_m is the proprioceptive-related internal model: basing on the muscle elongation to displace the manipulator, the pilot estimates the rate of change of the controlled element output. The pilot can do so because they have an internal/mental model of the controlled element dynamics: this is the equivalent of the equalization term discussed in the crossover

model, a term that depends on the controlled element and whose goal is to provide an open-loop desired slope of −20 dB/dec around the crossover frequency. T_2 can be considered equal to T_1, and k is the order of the controlled element dynamics in the crossover region. Being $u_m(t)$ an estimate of the output rate due to control activity u_δ, this loop is a form of rate feedback in the model. This aspect will be further discussed in the revised structural model section.
The internal model can be considered as a primary source of remnant: if the pilot has an inaccurate internal model, they will generate a command which is not precisely linear with respect to the real controlled element dynamics.

Pros and cons In terms of utility, the model shows more potential in the area of data interpretation rather than in prediction. Indeed, some of the parameters, the ones not already explicated in this text, must be tuned by means of real-world observations with the methods illustrated by Hess[4] , and there is not a simplified and fixed rule for each of them.
However, this model was worth mentioning because it is the father of two simplified models which are explicitly designed for simulation purposes.
This model is suitable only for single-loop single-axis compensatory tasks.

2.2.2 The revised structural model

In 1995, Hess[6] formulated the revised structural model, illustrated in Figure 8.

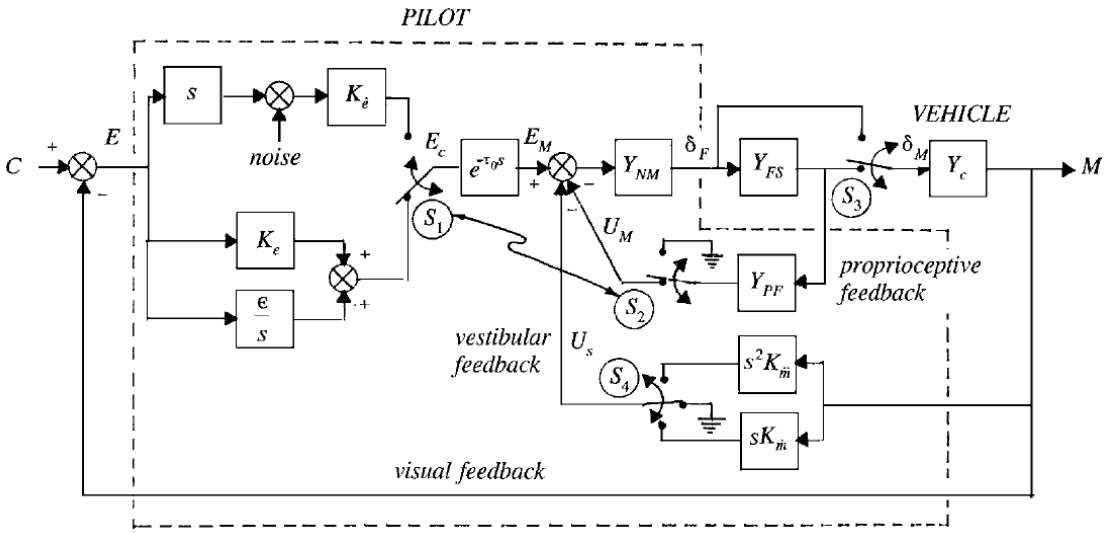

Figure 8: The revised structural pilot model

This model encompasses three sensory modalities: visual (sensing the error/error rate - switch S_1 - from the display visual input), vestibular (sensing the output rate/acceleration - switch S_4 - by means of the ear motion sensory system), proprioceptive (sensing the manipulator motion in order to create a signal proportional to the output rate due to manipulator motion - switch S_2).
The switch S_3 depends on the manipulator model Y_{FS}: if it is force sensing (the output is a force) the switch is up, if it is displacement sensing (the output is a displacement) the switch is down.
The switch S_1, that switches between rate and error type control, is associated with switch S_2: during a steady maneuver, the pilot actuates an error control and activates the proprioceptive feedback to perform equalization; at the beginning of a new maneuver, during the unsteady transition phase, the pilot does not possess an internal controlled element model, so they actuate a provisional rate control aimed at keeping the neutral stability, without the proprioceptive feedback. Therefore in a general simulated maneuver, for the sake of simplicity switch 1 and 2 can stay in the position associated with error control.
The spindle feedback dynamics that closed the neuromuscular loop in the structural model, here is neglected because it is very fast.

Parameters selection rules Here are some practical rules to tune the parameters and gains of the revised structural model:

Rule 1: position of the switches. The switches must be positioned according to the situation that is represented as explained above. In a first approximation, the vestibular feedback can be neglected.
Rule 2: fixed parameters. As justified in the structural model section, $\omega_{NM} = 10$ rad/s, $\xi_{NM} = 0.707$ and τ_0 can have a value of about $0.14s$.
Rule 3: proprioceptive feedback. Y_{PF} is the equalization term, which can have one of the following forms depending on the controlled element dynamics:

$$Y_{PF} = k(s + a) \quad \texttt{or} \quad Y_{PF} = k \quad \texttt{or} \quad Y_{PF} = \frac{k}{(s + a)} \tag{8}$$

The form of Y_{PF} can be set according to the crossover model rule:

$$\frac{Y_c(s)}{Y_{PF}(s)} = \frac{G}{s} \tag{9}$$

where G is a generic constant. According to Equation 9, $Y_{PF} \propto sY_c$, but, referring to Figure 8, $Y_c(s) = \frac{M}{\delta_M}$, therefore $sY_c(s) = \frac{\dot{M}}{\delta_M}$. The proprioceptive block is therefore an internal model of the transfer function from the manipulated variable to the controlled element output rate, as anticipated in the structural model section: it is a form of rate feedback.
The gain k appearing in Equation 8 is chosen so that, with all other loops open, the minimum damping ratio of any quadratic closed-loop poles of $\left(\frac{\delta_M}{E_M}\right)(s)$ is $\xi_{min} = 0.15$.

Rule 4: pilot gain tuning. K_e is selected so that the desired crossover frequency of 2 rad/s is obtained. The reasons why this crossover frequency has been used are detailed in another paper by Hess.[5]

Pros and cons This model is easier to tune and to use in simulations with respect to the structural model, and it is more precise in the representation of human dynamics than the crossover model. The fact that a fixed crossover frequency and a fixed inner-loop mimimum damping ratio were selected is not found to compromise particularly the fidelity of simulations.
This model was tested and proved to be reliable only for single-axis and single-loop compensatory tasks.

2.2.3 A simplified multi-loop structural model

In 2006, Hess[7] published an application of a simplified structural model with multi-loop capabilities and suited for pursuit display tasks.
Multi-loop in this case means that the pilot is not controlling directly the attitude, but a higher level variable: for instance, the pilot is controlling the position in hovering flight.
The proposed model is a simplification of the structural model, in which a rate feedback takes the place of the proprioceptive feedback, for the aforementioned interpretation of the proprioceptive feedback as a form of rate feedback. The structure of the primary loop (attitude control) model can be observed in Figure 9, while the structure of the multi-loop (high level variables) model is shown in Figure 10, which contains the primary loop of Figure 9.
To specify the figures to the longitudinal position hold in hovering flight: in Figure 9 M would be the pitch attitude, $\dot{M}$ would be the pitch rate; C of both Figures 9 and 10 is the commanded pitch attitude; in Figure 10 R_0 would be the commanded longitudinal speed, $\dot{M}_0$ the longitudinal speed, M_0 the longitudinal position, C_0 the commanded longitudinal position.

The model does not explicitly take into account the vestibular cues, in the sense that it is not specified how the feedback variables are sensed: if some feedback variable is an acceleration, it will be most probably sensed by means of the vestibular system.
The simplified structural model is suited to pursuit tasks for no particular theoretical or analytical reason, but because experimental data suggested a strong correlation with pursuit tasks at all frequencies, while for the compensatory tasks there is a divergence in the low frequency phase.

Parameters selection rules *Rule 1: neuromuscular dynamics*. G_{nm} is the neuromuscular transfer function, it can be treated as a second order transfer function by neglecting the high frequency spindle feedback dynamics. The neuromuscular dynamics is described by Equation 10:

$$G_{nm} = \frac{10^2}{s^2 + 2(0.707)10s + 10^2} \tag{10}$$

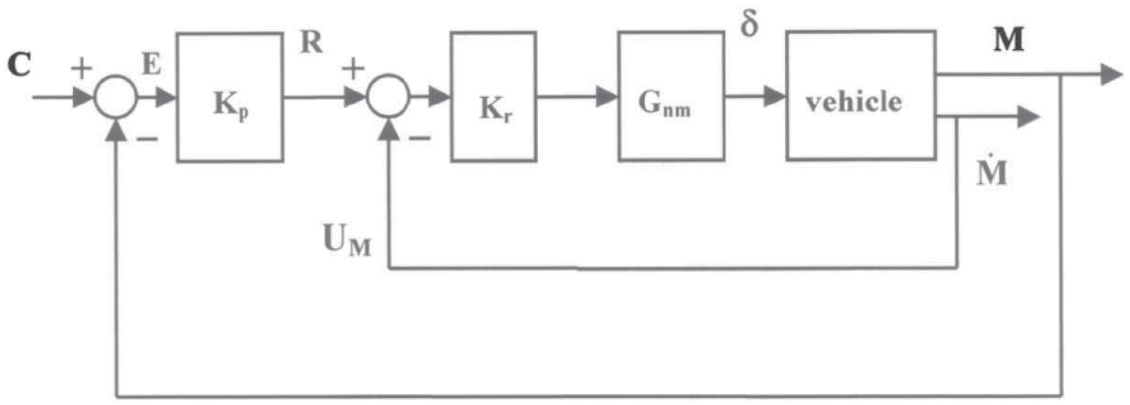

Figure 9: The simplified structural model

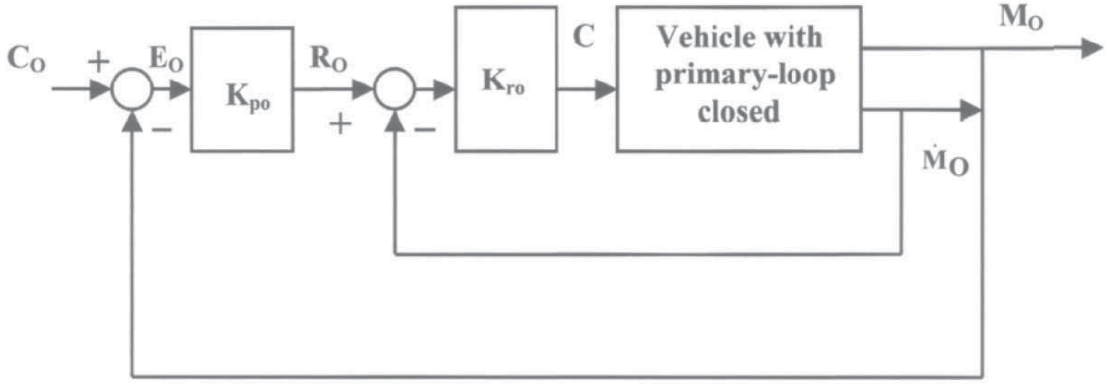

Figure 10: The multi-loop simplified structural model

where, as already discussed in the previous sections, $\omega_{nm} = 10$ rad/s and $\xi_{nm} = 0.707$.
Rule 2: K_r. The primary inner-loop gain is chosen as the gain value that results in a minimum damping ratio of $\xi_{min} = 0.15$ for any oscillatory mode in the inner closed-loop transfer function $\dot{M}/R$.
Rule 3: K_p. The primary outer-loop gain is chosen to provide a desired open-loop crossover frequency of 2 rad/s.
Rule 4: K_{r0}. The secondary inner-loop gain is chosen as the gain value that results in a crossover frequency for the transfer function $K_{r0}[\dot{M}_0/C]$ equal to the adjacent inner-loop crossover frequency (2 rad/s).
Rule 5: K_{p0}. The secondary outer-loop gain is chosen to provide a desired open-loop crossover frequency for the transfer function M_0/E_0 of one-third the value of the primary inner-loop crossover frequency: the secondary open-loop crossover frequency will be $2/3$ rad/s = 0.667 rad/s.

Pros and cons This model is suited for computer simulations, easy to tune and to apply. Moreover, it is a multi-loop and multi-axis model (multiple closed-loops can be applied on each axis), therefore very useful for aeronautical applications where there is the need of multi-axis control. However, the axes should be decoupled in order to apply this structure to multiple axes: the inter-axes coupling is neglected.

2.3 Frequency domain: mixed approach

After the elaboration of the crossover model, some models were developed to incorporate some of the human dynamics into the crossover law, in order to cover a broader frequency range. These types of models are not strictly iso-morphic or behavioral, but have some aspects of both the fashions.

2.3.1 The precision model

The precision model was developed by McRuer and is illustrated in the AGARD document.[14] This model, shown in Figure 11, incorporates the already discussed neuromuscular dynamics, and some central processing elements, such as

the central processing and computational delay, and four parallel channels which can be combined in order to obtain the equalization term of the crossover model.

In practice, the pilot simultaneously uses at most two of the four channels, and never uses the acceleration channel,

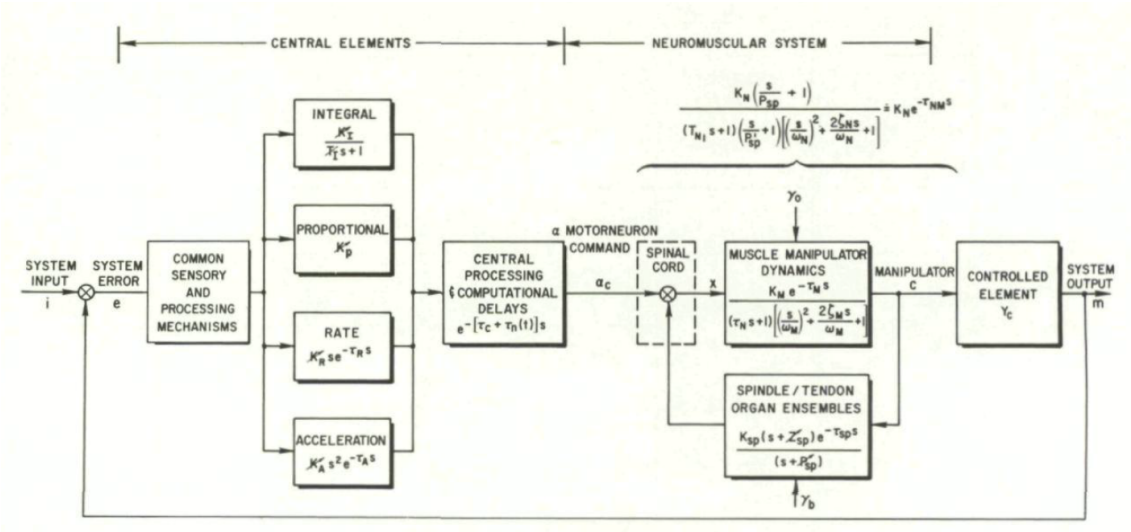

Figure 11: The precision model

therefore the general equation for the precision model is:

$$Y_p(s) = K_p \frac{\tau_p s + 1}{T_p s + 1} \frac{1}{\frac{s^2}{\omega_{NM}^2} + \frac{2\xi_{NM}}{\omega_{NM}} s + 1} exp(-\tau s) \tag{11}$$

The equalization time constants are tuned according to the crossover law; the pilot gain is set in order to have the desired crossover frequency of 2 rad/s as discussed for the structural model; the other parameters can be treated as constants and their values were established in the previous sections of this paper.

2.3.2 The Tustin-McRuer model

The Tustin-McRuer model[8] is a simplification of the precision model: the oscillating dynamics of the neuromuscular model is replaced by a first order dynamics, which constitutes a sufficiently accurate approximation of the pilot's response because the neuromuscular dynamics is at a significant higher frequency with respect to the crossover frequency.

The Tustin-McRuer model is one of the most widely used models, and is represented by the following equation:

$$Y_p(s) = K_p \frac{\tau_p s + 1}{(T_p s + 1)(T_{NM} s + 1)} exp(-\tau s) \tag{12}$$

The neuromuscular time constant can be set to $T_{NM} = 0.1\ s$.

2.3.3 The Gross model

The Gross model[8] is another simplification of the precision and Tustin-McRuer models, where the neuromuscular dynamics is modeled as a simple delay $\tau_{NM} = 0.1\ s$:

$$Y_p(s) = K_p \frac{\tau_p s + 1}{T_p s + 1} exp(-(\tau + \tau_{NM}) s) \tag{13}$$

2.4 Time domain: algorithmic

The first description of the behaviour of the human pilot in a time domain optimal control framework is due to Kleinman, Baron and Levinson[9] and dates back to 1970. Their research on the human pilot as an optimal controller is based upon the assumption that the well-trained and motivated human behaves optimally, apart for some inevitable human limitations.

2.4.1 OCM: the optimal control model

The system dynamics is represented by the linearized equations of motion, where $w(t)$ is the external disturbance modeled as a white noise, u is the control input and x is the state vector:

$$\dot{x}(t) = Ax(t) + Bu(t) + w(t) \tag{14}$$

The optimal control model is based on the assumption that the pilot chooses the control input in such a way to minimize the quadratic cost function:

$$J(u) = \lim_{T\to\infty} E\left(\frac{1}{T}\int_0^T (x^T Qx + u^T Ru + \dot{u}^T G\dot{u})\, dt\right) \tag{15}$$

The first term in the integral is the penalization on the state error, and the second term is the penalization on the control effort. This quadratic cost function presents also a third term, which is dependent on the control input rate. Kleinman, Baron and Levinson[9] showed that the control law obtained from minimizing the cost function $J(u)$ is:

$$\begin{aligned} \tau_n \dot{u}(t) + u(t) &= u_c(t) + v_u(t) \\ u_c(t) &= -L^* \hat{x}(t) \end{aligned} \tag{16}$$

where L^* is a matrix that depends on the solution of the associated Riccati equation and on the matrix G (all the equations are shown in detail and discussed in the optimal control model reference[9]). τ_n can be interpreted as the neuromotor lag, obtained by including the control rate in the cost function: appropriate values of τ_n can be obtained by appropriate choices of the G matrix weights. $v_u(t)$ is the control noise, intended as the noise introduced by the pilot while exerting the control action.
$\hat{x}(t)$ is the estimated state: the state can be estimated from the output by means of a generic estimator, but the output observed by the pilot is affected by an observation noise and by a time delay due to display lags or human perception delays, as indicated in Equation 17.

$$y_{obs}(t) = y(t-\tau) + v_y(t-\tau) \tag{17}$$

It has been found that the best solution to obtain an estimate of the state is to create a cascade of a Kalman filter, to obtain $\hat{x}(t-\tau)$ from $y_{obs}(t)$, and a least mean-squared predictor, to compute $\hat{x}(t)$ from $\hat{x}(t-\tau)$.
The complete optimal control model is illustrated in Figure 12.

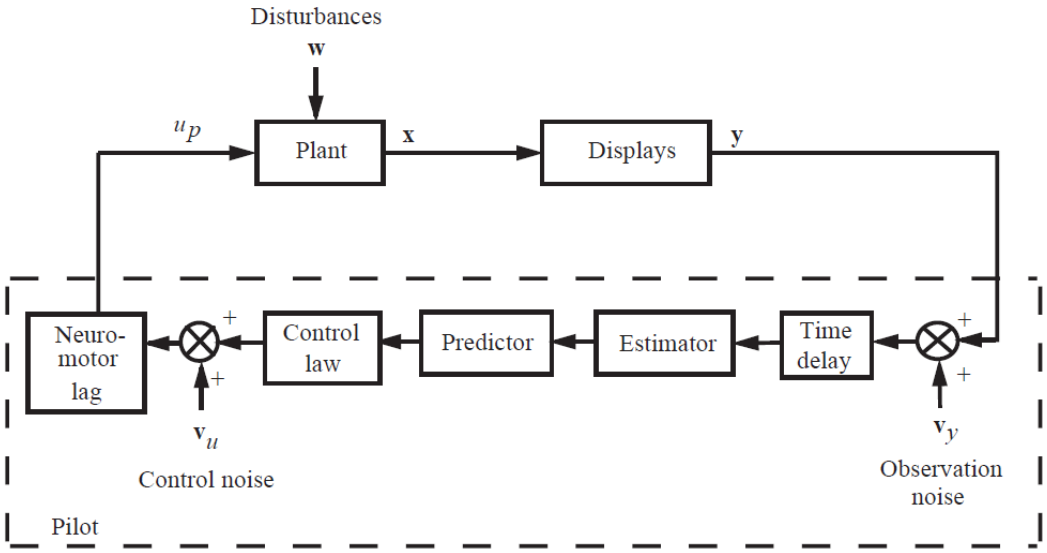

Figure 12: Block diagram of the optimal control pilot model

Pros and cons The main advantage of the time-domain OCM with respect to the frequency-based models is that, once the controlled element state-space linear equations are known, it is possible to create a pilot model: the algorithm just needs the state-space equations, independently on multiple closed loops, or multi-axes control. The OCM algorithm is therefore more flexible and suitable to a lot of different human-machine interaction structures. For instance, the OCM allows to treat also the inter-axis couplings.
On the other side, the settings of the weights in the cost function is not straightforward: there must be a careful analysis and knowledge of the problem.

2.4.2 MOCM: the modified optimal control model

The modified optimal control model was developed in 1992 by Davidson and Schmidt,[2] and it contains slight modifications of the optimal control model.
Differently from the OCM, the pilot's effective time delay is introduced after the pilot control action as a Pade second-order approximation, which augments the plant dynamics by two states. In this way, there is no need for the predictor after the Kalman filter, because the output measurement observed by the pilot is not delayed.
Appropriate values of the neuromotor lag τ_n are obtained by appropriate choice of control-rate weighting: to achieve the desired neuromotor time constant, iterations on the cost function control-rate weighting are usually required, as illustrated by the feedback in Figure 13, which contains the block diagram of the modified optimal control model.

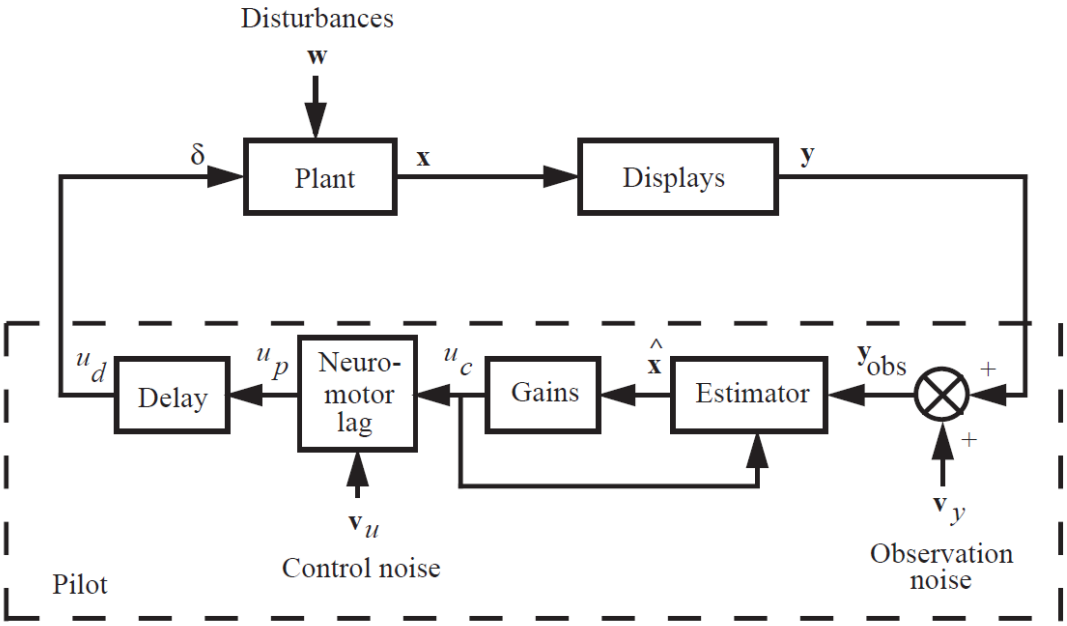

Figure 13: Block diagram of the modified optimal control pilot model

Pros and cons The major difference between the OCM and MOCM is the replacement of the linear predictor of the OCM by the augmentation of the system dynamics with the pilot's effective time delay. This difference allows for the direct calculation of the pilot and system transfer functions in the pole-zero form, which can be useful to perform frequency analyses.

2.4.3 ROCM: the revised optimal control model

In 2008, Wang et al.[17] proposed a revised optimal control model specific for computer simulations: differently from the OCM and MOCM, the ROCM, illustrated in Figure 14, does not model the neuromotor lag as a control-rate term in the cost function, but models the second-order neuromotor dynamics incorporating it in the plant dynamics. Therefore here the optimal control cost function is dependent only on the state error and control effort.
Similarly to the MOCM, the cortical processing delay is modeled by a Pade approximation, but in the ROCM also the visual perceptual cue dynamics is accounted for, and modeled again as a Pade approximation.

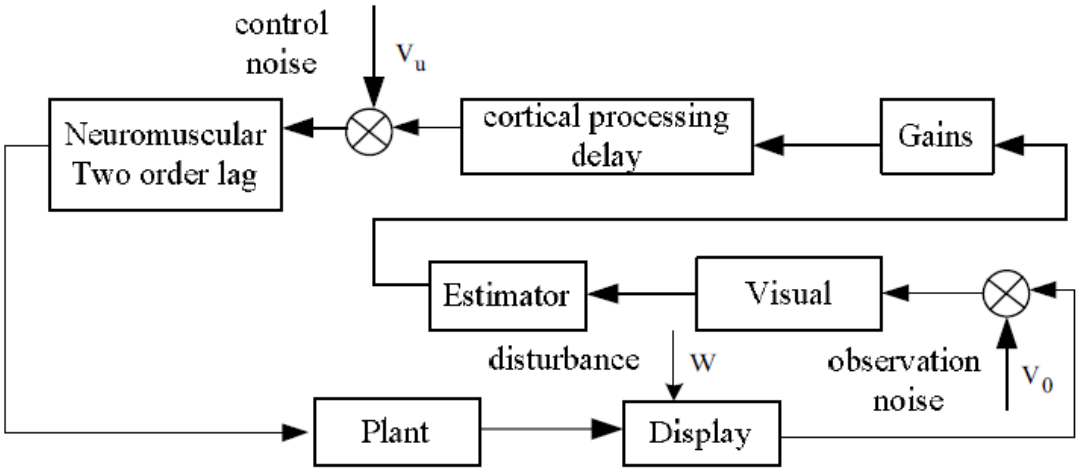

Figure 14: Block diagram of the revised optimal control pilot model

Pros and cons With respect to the OCM and MOCM, the ROCM has the main advantage of not needing to guess the cost function control-rate weighting in order to obtain an acceptable neuromotor lag.

3. Conclusions

The most used, validated and reliable human pilot behaviour models have been presented and compared in this paper. The main focus in this review has been on models of the human pilot as an active controller in order to perform closed-loop computer simulations.
The observations discussed for each model are summarized in Table 1, which contains an evaluation of: the type of display suited for the model (compensatory or pursuit); the capability of the model to represent multi-loop control (yes/no); the capability of the model to represent multi-axes control (yes/no); the capability of the model to represent inter-axis coupling situations (yes/no); the ease of gains tuning and implementation in computer simulations (easy/medium/hard).

Table 1: Summary of the characteristics of the pilot models

	Display	**Multi-loop**	**Multi-axis**	**Inter-axis coupling**	**Implementation**
Crossover	Compensatory	No	No	No	Easy
Structural	Compensatory	No	No	No	Hard
Revised structural	Compensatory	No	No	No	Medium
Simplified structural	Pursuit	Yes	Yes	No	Easy
Precision	Compensatory	No	No	No	Easy
Tustin - McRuer	Compensatory	No	No	No	Easy
Gross	Compensatory	No	No	No	Easy
OCM	Both	Yes	Yes	Yes	Medium
MOCM	Both	Yes	Yes	Yes	Medium
ROCM	Both	Yes	Yes	Yes	Easy

All the models treated in this paper are suitable for linear controlled elements, which can be expressed by means of a transfer function or a state space representation. The time-domain algorithms are more adaptable, because, even if the parameters in the controlled element state space change during the simulated task, the algorithm can minimize the cost function according to the new parameters, and find new pilot gains online. The frequency-based models, on the other hand, need a more articulated computation based on the rate inner-loop damping and open outer-loop crossover frequency and slope, which makes them more suitable to be characterized offline.
Currently, there are attempts to model pilots who control nonlinear controlled elements, which provide a better representation of reality, based on neural networks, but they are beyond the scope of this dissertation.

References

[1] Arrigo Avi, Nicola Frisco, Mattia Giurato, Marco Lovera, Pierangelo Masarati, Simone Panza, Gianluca Parnesari, Francesca Roncolini, Michele Sesana, Giuseppe Quaranta, et al. Scout drone: a drone-helicopter collaboration to support hems missions. In *48th European Rotorcraft Forum (ERF 2022)*, pages 1–8, 2022.

[2] John B Davidson and David K Schmidt. Modified optimal control pilot model for computer-aided design and analysis. Technical report, 1992.

[3] Ronald A Hess. A rationale for human operator pulsive control behavior. *Journal of Guidance and Control*, 2(3):221–227, 1979.

[4] Ronald A Hess. Structural model of the adaptive human pilot. *Journal of guidance and control*, 3(5):416–423, 1980.

[5] Ronald A Hess. Analysis of aircraft attitude control systems prone to pilot-induced oscillations. *Journal of Guidance, Control, and Dynamics*, 7(1):106–112, 1984.

[6] Ronald A Hess. Unified theory for aircraft handling qualities and adverse aircraft-pilot coupling. *Journal of Guidance, Control, and Dynamics*, 20(6):1141–1148, 1997.

[7] Ronald A Hess. Simplified approach for modelling pilot pursuit control behaviour in multi-loop flight control tasks. *Proceedings of the Institution of Mechanical Engineers, Part G: Journal of Aerospace Engineering*, 220(2):85–102, 2006.

[8] Miroslav Jirgl, Marie Havlikova, and Zdenek Bradac. The dynamic pilot behavioral models. *Procedia Engineering*, 100:1192–1197, 2015.

[9] David L Kleinman, S Baron, and WH Levison. An optimal control model of human response part i: Theory and validation. *Automatica*, 6(3):357–369, 1970.

[10] RE Magdaleno and MC RUER. Experimental validation and analytical elaboration for models of the pilot's neuromuscular subsystem in tracking tasks(experimental validation and analytical elaboration for models of pilot neuromuscular subsystem in tracking tasks). 1971.

[11] John R Mayo. The involuntary participation of a human pilot in a helicopter. 1989.

[12] Duane McRuer. Human dynamics in man-machine systems. *Automatica*, 16(3):237–253, 1980.

[13] Duane T McRuer and Henry R Jex. A review of quasi-linear pilot models. *IEEE transactions on human factors in electronics*, (3):231–249, 1967.

[14] Duane T McRuer and Ezra S Krendel. Mathematical models of human pilot behavior. Technical report, ADVISORY GROUP FOR AEROSPACE RESEARCH AND DEVELOPMENT NEUILLY-SUR-SEINE (FRANCE), 1974.

[15] GD Padfield. Rotorcraft virtual engineering; supporting life-cycle engineering through design and development, test and certification and operations. *The Aeronautical Journal*, 122(1255):1475–1495, 2018.

[16] Giuseppe Quaranta, Stefan van't Hoff, Michael Jones, Linghai Lu, and Mark White. Challenges and opportunities offered by flight certification of rotorcraft by simulation. 2021.

[17] Chunguang Wang, Feng Liao, Junwei Han, and Guixian Li. A revised optimal control pilot model for computer simulation. In *2008 2nd International Conference on Bioinformatics and Biomedical Engineering*, pages 844–848. IEEE, 2008.